3B.2. Environment and early evolution of the 8 May 2009 "Super Derecho"

Stephen F. Corfidi*[1], Michael C. Coniglio [2], and John S. Kain [2]

[1] NOAA/NWS/NCEP Storm Prediction Center, Norman, Oklahoma
[2] NOAA/OAR National Severe Storms Laboratory, Norman, Oklahoma

1. INTRODUCTION

This study documents the complex environment and early evolution of the remarkable derecho-producing convective system that crossed part of the central United States on 8 May 2009 (Fig. 1a). The derecho (Johns and Hirt 1987) severely damaged buildings, utility lines, and trees over a widespread area from western Kansas to eastern Kentucky as a result of multiple wind gusts > 35 m s^{-1} and isolated gusts > 45 m s^{-1} (Fig. 1b). The associated mesoscale convective system (MCS; Zipser 1982) contained bow echoes (Fujita 1978) during part of its lifetime, and an intense, long-lived mesoscale convective vortex (MCV; Davis and Trier 2007) developed during the latter stage of the MCS that was associated with very severe surface winds and tornadoes (Fig. 1). In addition, multiple tornadoes and localized swaths of intense wind damage occurred in association with strong meso-g scale (Orlanski 1975) vortices (Atkins and St. Laurent 2009) along the convective line, as found for other extreme damaging-wind MCSs (Miller and Johns 2000; Wheatley et al. 2006).

The 8 May 2009 MCS developed in a way that is common to similar systems that affect the central United States during spring. Convective initiation occurred along the eastern slopes of the Rocky Mountains, and storms subsequently moved east to consolidate in a region of lower-tropospheric warm advection, convergence, and conditional instability in the exit region of a nocturnal low-level jet (LLJ) (Blackadar 1957; Bonner 1968; McNider and Pielke 1981; Cotton et al. 1989; Laing and Fritsch 2000; Tuttle and Davis 2006). The development of a large, intense MCS resulted from a complex series of processes and mergers of several convective lines and clusters over a relatively short time period, which is common for warm season MCSs (McAnelly et al. 1997; Jirak and Cotton 2003).

Routine surface and upper air observations and analyses from the Rapid Update Cycle (RUC; Benjamin et al. 2004) are used in this study to determine what, if anything, was unusual about the environment over the central plains on 8 May 2009. In particular, analyses from this event are compared to those from other MCSs that have occurred over much the same region and time of year. Although the genesis and evolution of the MCV was a significant part of this event, the focus here is on the environment and early evolution of the convective system prior to the development of the MCV. We emphasize the system's early evolution since it is likely that the ability to accurately predict convective systems of this type is strongly related to a detailed understanding of the processes and environmental ingredients that can create such a system.

* *Corresponding author address:* Stephen F. Corfidi, NOAA/NWS/NCEP/Storm Prediction Center, 120 D. L. Boren Blvd., Norman, OK 73072; email: stephen.corfidi@noaa.gov

2. DATA AND METHODOLOGY

Our analysis of the 8 May 2009 convective system makes use of radar data from the National Weather Service Weather Surveillance Radar-1988 Doppler (WSR-88D) network. This analysis includes level II data from individual WSR-88D sites obtained from the National Climatic Data Center, base reflectivity composites generated by Unisys, and composite (column-maximum) reflectivity derived from the National Mosaic and Multi-sensor Quantitative precipitation estimation (NMQ) project (Vasiloff et al. 2007). In addition, this study uses surface and upper-air observations from a variety of platforms that were quality controlled by the NOAA Meteorological Assimilation Data Ingest System (MADIS) (see Fig. 2 for site locations of the radiosonde, wind profiler, and WSR-88D data used in this study). These data are used to document the complex development and early evolution of the convective event.

The MCS environment is further examined using the hourly RUC-model analyses provided on a 20-km grid and on constant pressure surfaces spaced 25 hPa apart. To address the question of what was unusual about the environment, the RUC analysis of the 8 May 2009 event is compared to those from 28 MCSs obtained from the dataset described in Coniglio et al. (2010) [referred to as C2010 hereafter]. This comparison dataset includes MCSs that occurred from early May to early June in the central U.S. and that had a nearly contiguous reflectivity region ≥ 35 dBZ at least 100 km in length and embedded echoes ≥ 50 dBZ for at least five continuous hours. Although not all of the comparison MCSs produced derechos or

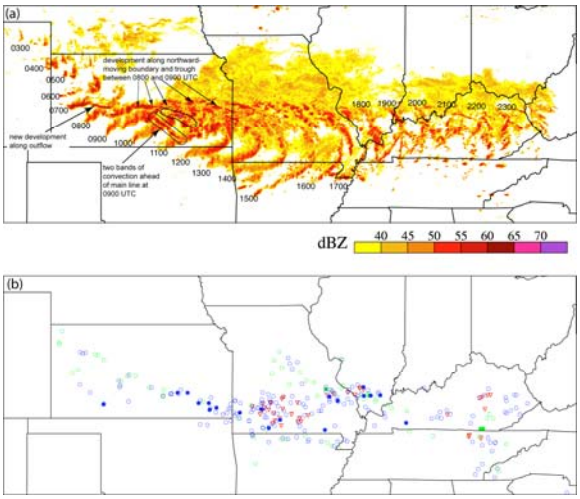

Figure 1. (a) Hourly composite reflectivity images from the NMQ project plotted at 1-hr intervals (UTC) and (b) severe weather reports associated with the derecho-producing MCS (hail ≥ 0.75 inches in open green circles, hail ≥ 2.0 inches in filled green circles, wind damage or wind gusts ≥ 26 m s^{-1}, or 50 kt, in open blue circles, wind gusts measured or estimated ≥ 33.5 m s^{-1}, or 65 kt, in filled blue circles, and tornado reports in red), from 0300 UTC to 2300 UTC 8 May 2009.

severe weather, all of them eventually transitioned into a leading line/trailing stratiform structure (Houze et al. 1989; Parker and Johnson 2000) that resembled the mature structure of the 8 May 2009 MCS.

In the C2010 study, changes in the environment relative to the location and movement of the MCSs are examined by producing composite RUC analyses at several stages in the MCS lifecycle, including the pre-deep-convection environment (termed the "first storms" stage in C2010) and the environment ahead of newly developed MCSs (termed the "genesis" stage in C2010). The environments at the time of the first storms' and genesis stages of the 8 May 2009 MCS are compared to the composite environments of the first storms' and genesis stages for the 28 other MCSs in the C2010 data set using standardized anomalies (a_s), where $a_s = (x_a - \mathbf{x})\sigma_s$ is calculated at each grid point, x_a is a grid point value of a variable x in the RUC analysis for the 8 May 2009 event, $\mathbf{x}$ is the mean of x from the C2010 MCS data set, and σ_s is the sample standard deviation of x from the C2010 MCS data set. The first storms' and genesis stages of the 8 May 2009 MCS are defined to be at 0300 UTC and 0700 UTC, respectively. Examination of the anomalies in this manner allows an investigation of what was unusual about the environment of the 8 May 2009 derecho compared to other MCS environments that occurred in a similar place and time of year.

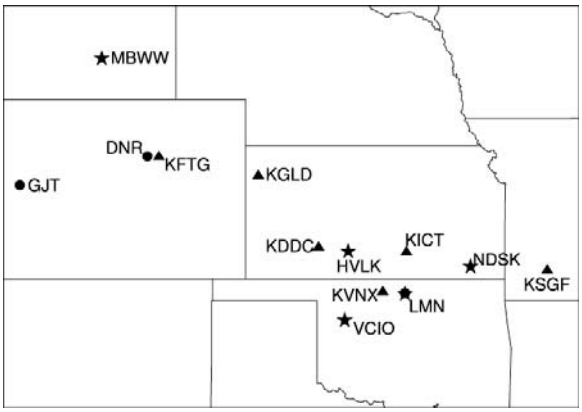

Fig. 2. Locations and names of the 915 MHz wind profiler sites (★),WSR-88D sites (▲), and radiosonde sites (●) used in this study.

3. ANALYSIS

a. Environmental conditions preceding development of deep convection

Relatively dry conditions and few clouds covered much of the central High Plains in the early afternoon of 7 May (Fig. 3a) beneath moderately strong westerly mid to upper level flow (Figs. 4 and 5). A band of cumuliform clouds developed over far northeast Colorado (Fig. 3a) near the western end of a surface trough that extended from a weak low over far eastern Nebraska. Cloud bases were relatively high, atop a well-mixed, relatively dry boundary layer (Fig. 4). Nearby WSR-88D radars detected light precipitation (mostly < 35 dBZ) with this initial cloudiness, much of which did not appear to reach the ground. The low CAPE likely limited the strength of the convection initially.

Vertical motion and potential temperature fields in vertical cross sections (not shown) suggest that mountain waves partially were responsible for the initial clouds and precipitation. Upstream conditions in which strong mountain waves are likely to develop are evident in the observed soundings at Grand Junction and Denver, Colorado (not shown), and in the nearby RUC sounding (Fig. 4). These conditions consist of (i) strong wind at mountain top level, increasing with height and oriented perpendicular to the mountain range throughout a deep layer, and (ii) a relatively stable layer near mountain top height with weaker stability at higher levels (Durran 1986). Furthermore, a local maximum in low-level westerly flow over the terrain in far southern Wyoming appears to enhance the convergence and upward motion locally over far southeastern Wyoming (not shown), where the shallow convection first appears.

The northeastern Colorado/southeastern Wyoming/Nebraska border region also was under the right entrance region of a mid-level jet streak (Fig. 5),

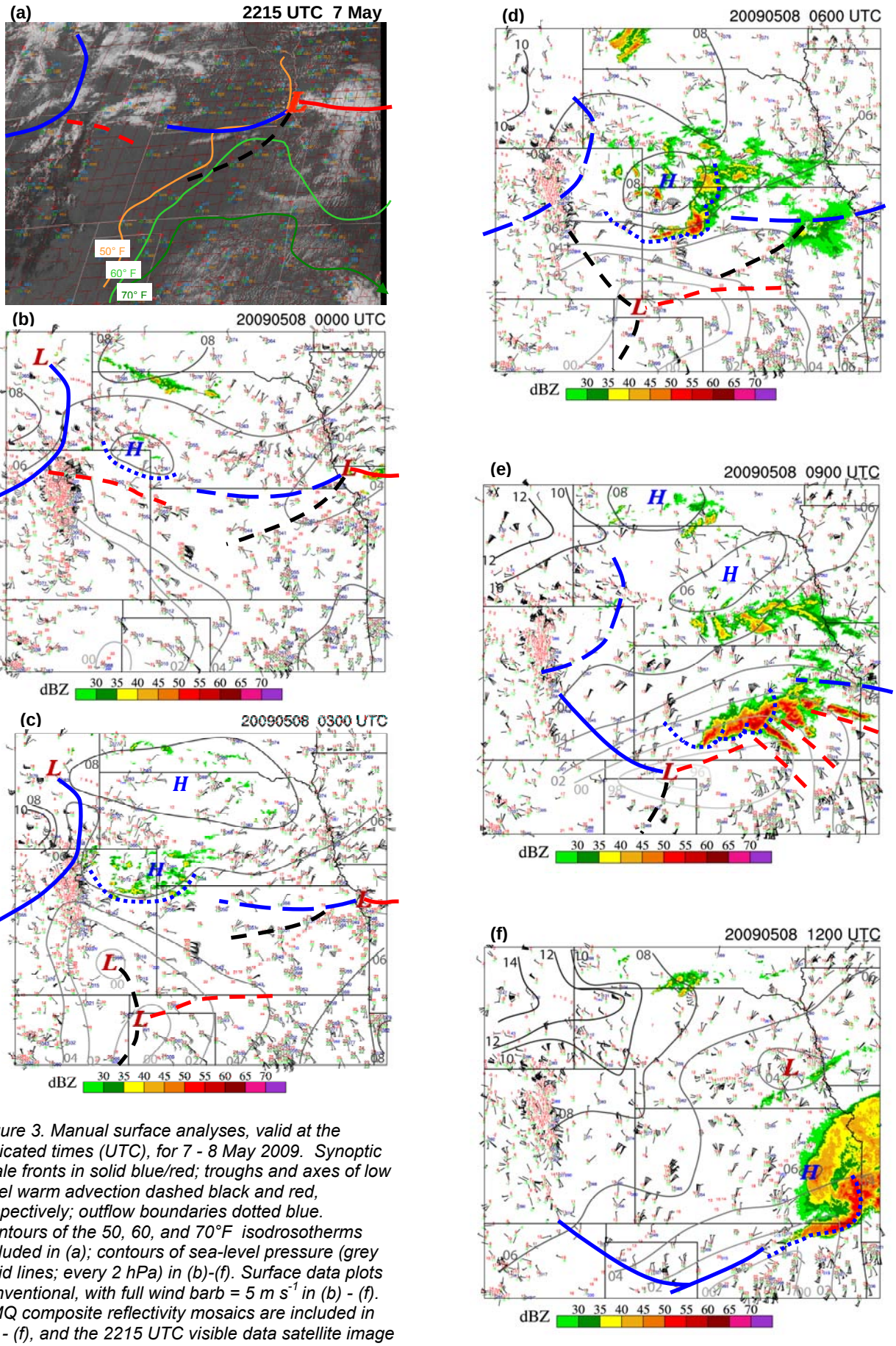

Figure 3. Manual surface analyses, valid at the indicated times (UTC), for 7 - 8 May 2009. Synoptic scale fronts in solid blue/red; troughs and axes of low level warm advection dashed black and red, respectively; outflow boundaries dotted blue. Contours of the 50, 60, and 70°F isodrosotherms included in (a); contours of sea-level pressure (grey solid lines; every 2 hPa) in (b)-(f). Surface data plots conventional, with full wind barb = 5 m s^{-1} in (b) - (f). NMQ composite reflectivity mosaics are included in (b) - (f), and the 2215 UTC visible data satellite image in (a).

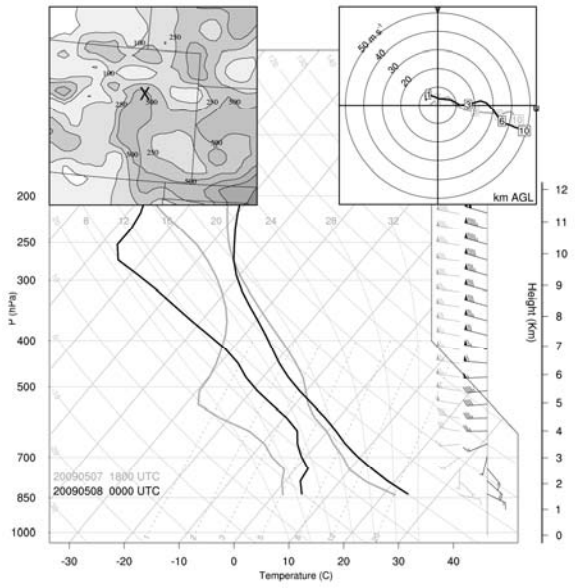

Fig. 4. Skew-T diagram of temperature and dewpoint and hodograph (inset in upper right) valid 1800 UTC 7 May 2009 (light grey lines and winds) and 0000 UTC 8 May 2009 (black lines and winds) from the RUC analysis at the location in northeast Colorado marked with the X in the upper-left inset. Half (full) barbs are drawn every 2.5 (5) m s^{-1} and pennants are drawn at 25 m s^{-1}. The inset in the upper left also shows the RUC analysis of MUCAPE (contours of 10, 100, 250, 500, and every 500 m^2 s^{-2} thereafter valid 0000 UTC 8 May.

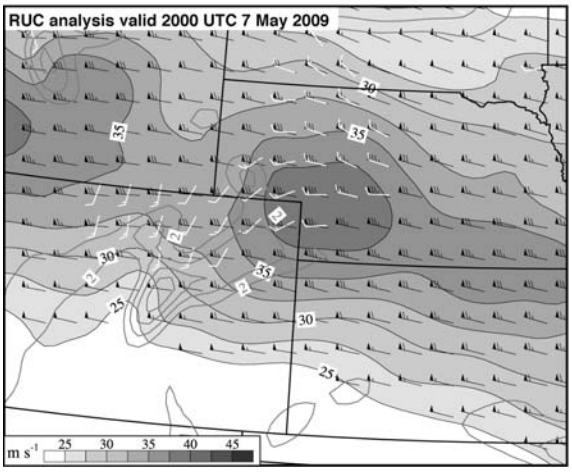

Fig. 5. RUC analysis of 450-hPa total wind, ageostrophic wind, and horizontal divergence valid at 2000 UTC 7 May 2009. Total wind speed is shaded every 2.5 m s^{-1} starting at 25 m s^{-1} and is represented by the black wind barbs. The white wind barbs represent the ageostrophic wind. Full wind barbs are drawn every 5 m s^{-1} and pennants represent 25 m s^{-1}. Horizontal divergence is contoured every 2 x 105 s^{-1} starting at 2 x 105 s^{-1} (grey lines).

which often is collocated with MCS development (Maddox 1983; Johns 1993; Coniglio et al. 2004). The flow is significantly ageostrophic in this region (Fig. 5), which may be the result of jet-streak dynamics (Uccellini and Johnson 1979) and lee-side flow deceleration associated with terrain-induced waves (Durran 1986). Furthermore, upslope flow and an associated "Denver cyclone" (Szoke et al. 1984) were evident in the surface observations and in WSR-88D level II data from Denver (not shown). Coincident with the Denver cyclone was the development of a weak mid-level vorticity maximum over the heated terrain of the Rockies in north central Colorado. Finally, the southern fringe of a mid-level shortwave trough traversing Wyoming approached the area and may have contributed to the lift by 0000 UTC 8 May. All of these factors likely contributed to the upward vertical motion and subsequent weak convective development in eastern Colorado and far southeast Wyoming by 0000 UTC (Fig. 3b).

After 0000 UTC on 8 May, weak convection continued to form over north central Colorado. A southwest-moving outflow boundary originating from this convection interacted with the Denver cyclone to help initiate convection over northeastern Colorado. Precipitation falling through the deeply-mixed boundary layer with very steep low-level lapse rates (Fig. 4) likely fostered the development of evaporatively cooled low-level air that expanded rapidly over northeastern Colorado through 0300 UTC (Fig. 3c).

b. Evolution of the environment and convection prior to MCS development

Much stronger convection developed shortly after 0300 UTC near the intersection of the outflow boundary and the pre-existing pressure trough over southern Yuma County in northeast Colorado. Although the convection was deeper, it likely continued to be high-based, as RUC analyses in this region showed lifting condensation levels generally over 2000 m AGL (Fig. 4). Furthermore, instability at this stage of MCS development was very low compared to the environments just prior to deep convective initiation for the 28 MCSs in the C2010 data set (Fig. 6). The largest values of most-unstable convective available potential energy (MUCAPE) were only 300 m^2 s^{-2} ahead of the first storms over far eastern Colorado and northwest Kansas (Fig. 6a). These values are less than two standard deviations below the mean MUCAPE for the 28 MCSs in the comparison data set (Fig. 6d). The low MUCAPE resulted from the lack of boundary-layer moisture and relatively weak mid-level lapse rates (Fig. 4).

The reasons why the convection intensified after 0300 UTC are not obvious, but there is evidence that the localized environmental conditions rapidly were becoming more favorable for strong convection. For example, the RUC analysis indicated an increase in horizontal convergence associated with the strengthening cold pool and strengthening southerly

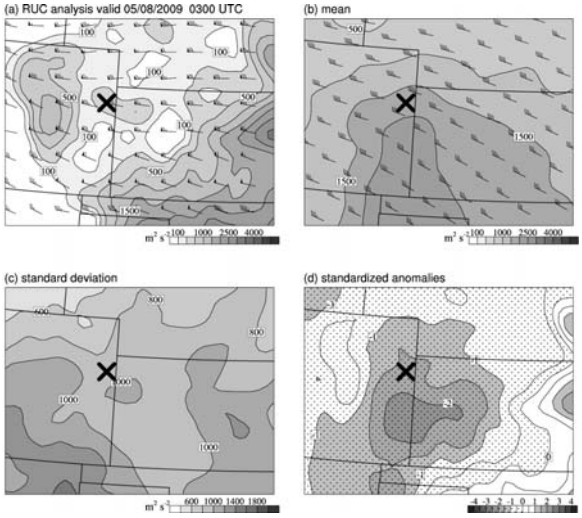

Figure 6. (a) RUC analysis of MUCAPE shaded and contoured with values of 100, 250, 500 $m^2 s^{-2}$, then every 500 $m^2 s^{-2}$ thereafter, and 0-6 km wind shear vectors (full barb = 5 m s^{-1}, pennant = 25 m s^{-1}). The X marks the location of the strong convective development shortly after 0300 UTC. (b) As in (a) except for the mean MUCAPE ahead of the first storms of developing MCSs from the set of 28 MCSs described in section 3, where the X marks the location of ensuing first-storms development that was used in the compositing procedure. (c) As in (b) except for the standard deviation of MUCAPE from the set of 28 MCSs shaded and contoured every 200 $m^2 s^{-2}$, and (d) MUCAPE standardized anomalies based on a comparison to the Coniglio et al. (2010) data set, with the negative anomalies hatched.

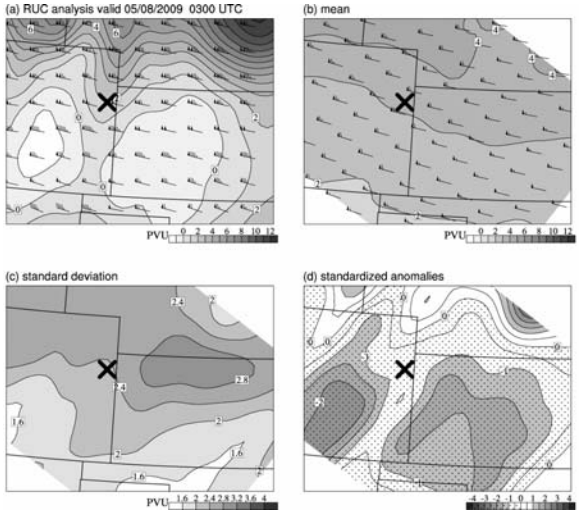

Figure 7. As in figure 6 except for geostrophic potential vorticity and geostrophic winds (full barb = 5 m s^{-1}, pennant = 25 m s^{-1}) on the 345 K potential temperature surface (1 PVU = 10-6 $m^2 s^{-1} K kg^{-1}$).

flow of higher equivalent potential temperature (θ_e) air aloft in the 1 – 2 km AGL layer (not shown). Furthermore, the dry sub-cloud air (Fig. 4) favored rapid development of cold pools. The stronger thunderstorms that developed after 0300 UTC persisted and moved east-southeast into northwest Kansas. Despite the limited instability, the strong westerly flow aloft created substantial 0 – 6 km vertical wind shear (Fig. 6a) that supported organized thunderstorms along the downshear side of the cold pool. These storms expanded south and east through 0600 UTC (Figs. 3c and 3d),

Furthermore, preceding deep-convective development, a large region of upper tropospheric negative geostrophic potential vorticity (PV_g) was found over western Kansas (Fig. 7a), where the deep convection subsequently grew upscale. Negative PV_g is a necessary condition for inertial instability on isentropic surfaces in a dry, gravitationally stable atmosphere. An atmosphere that is weakly stable (or unstable) inertially favors the efficient ventilation of convective outflow in the upper troposphere (Emanuel 1979; Seman 1994) and low values of PV_g may signal the rapid upscale growth of MCSs (Blanchard et al. 1998; Schultz and Knox 2007; C2010). Not only were the values of PVg low in an absolute sense, but also were low compared to the environments of other MCSs, with standardized anomalies in the -1.5 to -2 range (Fig. 7d). As hypothesized in Seman (1994) and Blanchard et al. (1998), weak ambient inertial stability is important to the development of deep mesoscale circulations that can support additional convection on the baroclinically warm side of the circulation (usually equatorward in the Northern Hemisphere). Presumably in the 8 May 2009 case, the efficient ventilation of updraft mass in the weak ambient inertial *instability* may have compensated for the relative lack of conditional instability initially.

The atmosphere was undergoing rapid changes by 0600 UTC in response to the development of a strong south-southwesterly LLJ over the Southern Plains. The jet tapped a reservoir of very moist air over western Oklahoma and the Texas panhandle. Low-level horizontal convergence (not shown) increased in the region ahead of the LLJ and south of the outflow boundary that extended west from the original convection (Figs. 3c and 3d). This enhanced low-level convergence likely aided the development of thunderstorms along the southward-surging outflow boundary in west central Kansas at 0600 UTC (Fig. 3d). After 0600 UTC, the convective outflow surged 20 – 30 km ahead of the weakening original convection. Explosive convection subsequently developed along the outflow boundary by 0700 UTC (Fig. 1a).

c. Mature MCS evolution between 0600 UTC and 1200 UTC

The evolution of convection after 0600 UTC was quite complex and is discussed here to illustrate the departure it represents from the simplified

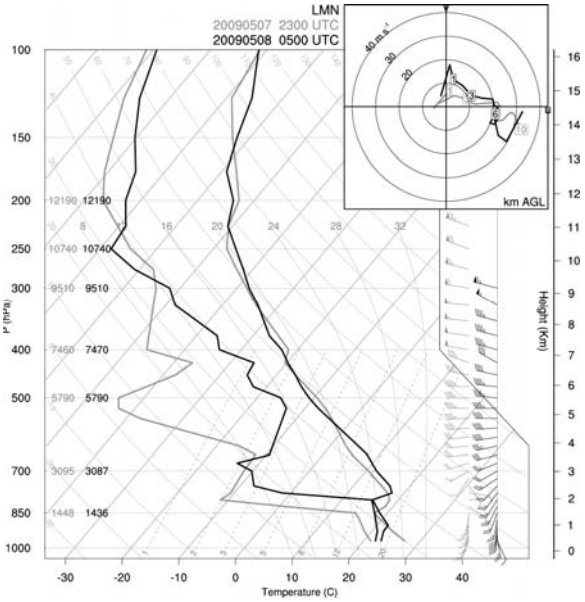

Figure 8. Skew-T diagrams and hodographs from observed soundings at Lamont, Oklahoma (LMN- see Fig. 2 for location) valid at 2300 UTC 7 May 2009 (grey lines) and 0500 UTC 8 May 2009 (black lines). Full wind barbs represent 5 m s^{-1} and pennants represent 25 m s^{-1}.

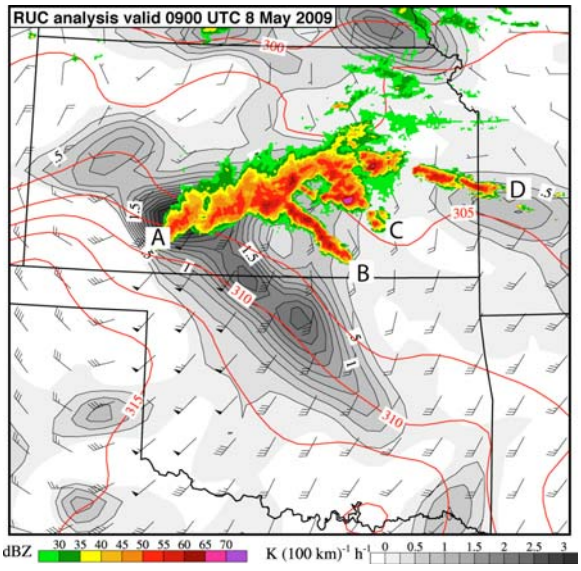

Figure 9. RUC analysis of 2D frontogenesis shaded and contoured every 0.25 K (100km)$^{-1}$ h^{-1}, wind vectors (full barb = 5 m s^{-1}, pennant = 25 m s^{-1}), and potential temperature (red contours every 2.5 K) on the 825-hPa surface valid 0900 UTC 8 May 2009, with NMQ composite reflectivity overlayed.

evolutions that commonly appear in MCS modeling literature. New thunderstorms formed along a northward moving boundary that appeared to be associated with a pressure trough extending east from a developing low pressure center over the

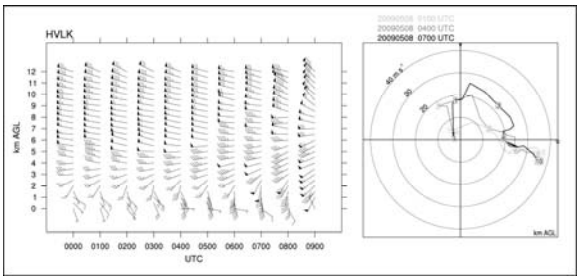

Figure 10. Hourly wind profile from Haviland, Kansas (HVLK) from 0000 UTC to 0900 UTC 8 May 2009. Full wind barbs represent 5 m s^{-1} and pennants represent 25 m s^{-1}; hodographs are valid 0100 UTC (light grey line), 0400 UTC (medium grey line), and 0700 UTC (black line). The 10-m wind from the nearest surface station was used for the surface wind. The MCS reached the HVLK site shortly after 0900 UTC.

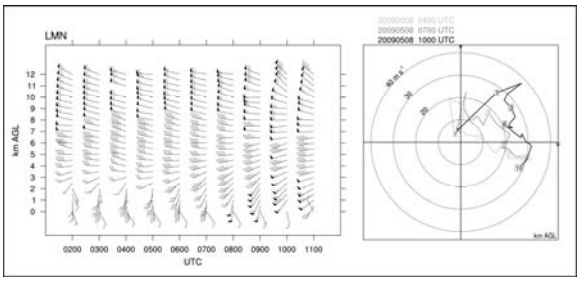

Figure 11. Hourly wind profile from Lamont, Oklahoma (LMN) from 0200 UTC to 1100 UTC 8 May 2009. Full wind barbs represent 5 m s^{-1} and pennants represent 25 m s^{-1}; hodographs are valid 0400 UTC (light grey line), 0700 UTC (medium grey line), and 1000 UTC (black line). The 10-m wind from the nearest surface station was used for the surface wind.

Oklahoma/Texas panhandles (Figs. 3d and 3e). The boundary also appeared to mark the sharpest gradient in moisture from the moderately moist air mass over south central Kansas to the very moist air farther south, as seen in a comparison of soundings taken at 2300 UTC 7 May and at 0500 UTC 8 May at Lamont (LMN) in north central Oklahoma (Fig. 8). Perhaps as a consequence of the rapidly strengthening and deepening low-level flow, the northward moving boundary appeared to sharpen with time in the WSR-88D level II data from Wichita, Kansas (not shown). This may have indicated an increase in horizontal convergence that helped initiate the convection along the boundary. After 0800 UTC, the boundary and the convection along it merged with the main area of thunderstorms farther west (labeled band "A" in Fig. 9). Shortly thereafter, additional storms formed along the preexisting trough over east central Kansas (shown in Fig. 3), merged with the other areas of convection, and expanded eastward to the Kansas/Missouri border by 0900 UTC (the easternmost segment labeled “D” in Fig. 9).

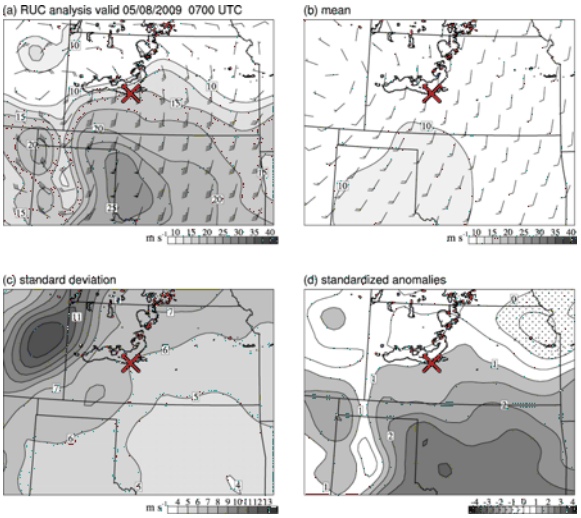

*Figure 12. (a) RUC analysis of 500-m AGL wind speed shaded and contoured every 2.5 m s^{-1}, starting at 10 m s^{-1} (full barb = 5 m s^{-1}, pennant = 25 m s^{-1}) valid 0700 UTC 8 May 2009. The **X** marks a location near the center of the leading convective line that was used for the comparison of the analysis to the Coniglio et al. (2010) data set. (b) As in (a) except for the mean 500-m AGL wind speed ahead of the newly-developed MCSs from the set of 28 MCSs described in section 3, where the **X** marks the location near the center of the leading convective line that was used in the compositing procedure. (c) As in (b) except for the standard deviation of 500-m AGL wind speed from the set of 28 MCSs shaded and contoured every 1 m s^{-1}, and (d) 500-m AGL wind speed standardized anomalies based on a comparison to the Coniglio et al. (2010) data set, with the negative anomalies hatched.*

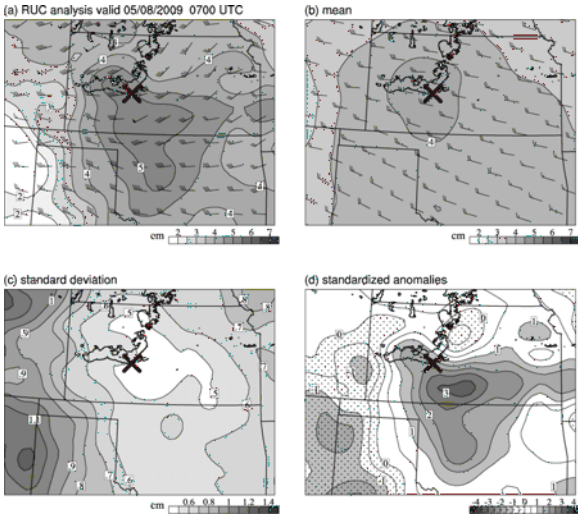

Figure 13. As in figure 12 except for the precipitable water (shaded and contoured every 0.5 cm) and 0-3 km wind shear vectors (full barb = 5 m s^{-1}, pennant = 25 m s^{-1}) valid 0700 UTC 8 May 2009.

Adding to the complexity of the convective development were two bands that formed ahead of the main convective line after 0800 UTC (labeled "B" and "C" in Fig 9). Examination of WSR-88D level II data revealed alternating bands of maxima and minima in clear-air reflectivity, and corresponding variations in radial velocity that were oriented perpendicular to the LLJ. These features propagated to the northeast (not shown), perhaps marking the "nose" or exit region of the LLJ. One of the better-defined clear-air reflectivity bands appeared to mark the transition in 2 km AGL wind from 15 m s^{-1} at 0600 UTC to 25 m s^{-1} at 0700 UTC as it passed the Haviland, Kansas (HVLK) profiler site (Fig. 10). Convective band "B" (Fig. 9) developed along this feature as it moved north and east. Likely aiding the convective development was the strong horizontal convergence and low-level deformation frontogenesis along the leading edge of the LLJ (Fig. 9). This conclusion is supported by the fact that bands "B" and "C" were aligned with the long axis of the frontogenesis (Fig. 9).

By 0900 UTC, the western half of band "A" had changed orientation from nearly east-west to southwest-northeast (Fig. 9). At this time, band "B" was expanding and intensifying, while band "C" was decreasing in coverage and intensity. The intersection of band "A" and band "B" formed a pivot point for the change in line orientation and marked the northern extent of a subsequent small-scale bow-echo and an area of mesovortices that produced wind gusts > 36 m s^{-1} and significant property damage in the vicinity of Wichita after 0900 UTC. The western half of the convective line developed a larger scale bow echo and accelerated to the east-southeast as the system became oriented more perpendicular to the west-northwesterly mid and upper level flow (Figs. 3e & 3f). This behavior is consistent with the idea that, as a cold pool consolidates, rapid downwind cell regeneration and propagation are favored along the portion of the outflow that becomes oriented perpendicular to a wind profile that is nearly unidirectional and contains shear over some depth of the troposphere (Weisman 1993; Corfidi 2003; Cohen et al. 2007).

After the development of the bow echo, numerous intense convective cells continued to form near the intersection of bands "A" and "B", where a very large area of nearly contiguous radar reflectivity echoes > 45 dBZ was concentrated over southeastern Kansas by 1000 UTC (Fig. 1a). Through 1200 UTC, the system accelerated and moved perpendicular to the mean deep-layer wind/shear and developed a larger-scale bow echo structure as it entered southwest Missouri after 1200 UTC. Ahead of the storms, the slightly backed flow in the 0.5 – 1.5 km layer was unusually strong (Figs. 10 and 11) and allowed for very efficient storm-relative inflow of very moist, unstable air that supported the continued regeneration of strong updrafts along the advancing cold pool (Fig. 3f)

d. Evolution of the LLJ

One of the remarkable characteristics of the environment of the 8 May 2009 derecho was that the

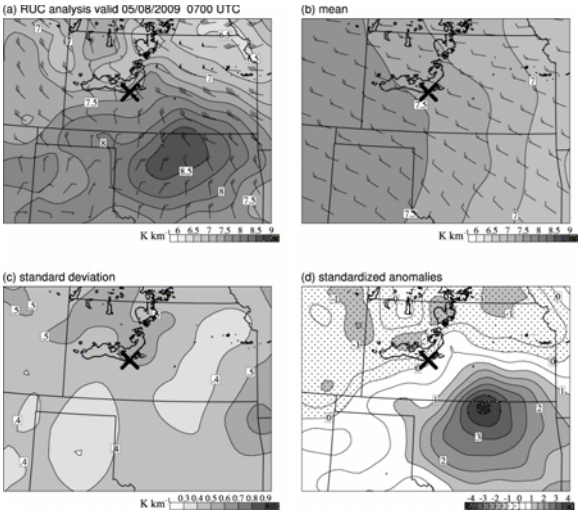

Figure 14. As in figure 12 except for the 3 – 6 km lapse rates (shaded and contoured every 0.25 K km^{-1}) and 3 – 6 km wind shear vectors (full barb = 5 m s^{-1}, pennant = 25 m s^{-1}) valid 0700 UTC 8 May 2009.

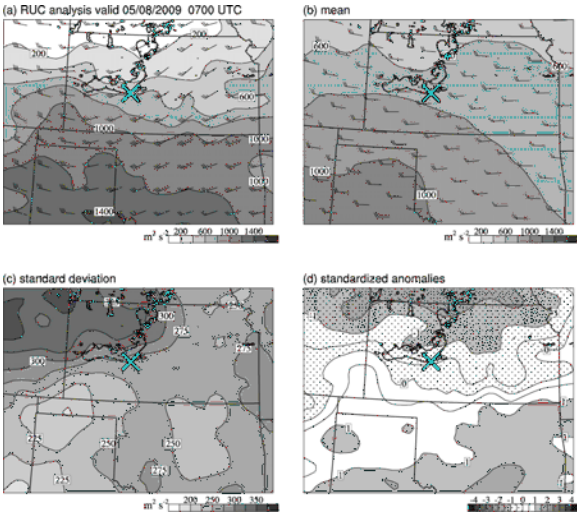

Figure 15. As in figure 12, except for DCAPE (shaded and contoured every 200 m2 s^{-2}) and 0 – 6 km mean wind vectors (full barb = 5 m s^{-1}, pennant = 25 m s^{-1}) valid at 0700 UTC 8 May 2009.

LLJ was both unusually strong and very deep. The weak winds at 2300 UTC in the 900-800 hPa layer at Lamont, Oklahoma were replaced with stronger southerly and southwesterly winds by 0500 UTC (Fig. 8). A deepening of the LLJ also is seen in the wind profile at Haviland, Kansas (Fig. 10). But the deepening is particularly evident at Lamont. There, the 3 km AGL flow increased from west-southwesterly at 10 m s^{-1} at 0400 UTC to southwesterly at 28 m s^{-1} at 1000 UTC (Fig. 11). The low-level wind speeds were measured as high as 38 m s^{-1} at 1000 UTC (at 1.5 km on Fig. 11), which further emphasizes the unusual strength of the LLJ for this event.

The Blackadar (1957) decoupling mechanism for LLJ formation usually confines the stronger wind speeds to near the top of the nocturnal boundary layer (McNider and Pielke 1981), which appeared to be below 1 km AGL (Fig. 8), so the explanation for this unusually deep LLJ likely lies elsewhere. The very deep LLJ could be related to (i) the coupling of the low-level southerly ageostrophic flow to the mid-level ageostrophic circulation and jet streak (Uccellini and Johnson 1979) that was moving across the area (not shown), (ii) the ageostrophic circulation associated with a band of frontogenesis crossing the region (Fig. 5), or (iii) the strengthening of the lee trough over the Texas/Oklahoma panhandles (Fig. 3). Regardless of the mechanism, the result was a deep mesoscale surge of strong, low-level flow across south-central Kansas, directed toward the developing convective system.

In addition to its unusual strength and depth, the LLJ was also very broad. At 0700 UTC, the time of MCS genesis, wind speeds at 500 m AGL were > 30 m s^{-1} in the wind profile at Vici in northwest Oklahoma (not shown), and were analyzed to be > 25 m s^{-1} over much of western Oklahoma (Fig. 12a). Furthermore, *500 m AGL wind speeds > 20 m s^{-1} covered much of Oklahoma and the Texas Panhandle, resulting in a large area of a_s > 2 over most of Oklahoma and peak values of a_s > 3 in some locations in the jet core (Fig. 12d)*. A strong and broad LLJ was anticipated by the short-term numerical forecast guidance, although not as strong or broad as revealed by observations and analyses.

e. Evolution of the thermodynamic environment after MCS development

Along with the strong surge of low-level southerly flow, the environment feeding into the developing MCS by 0700 UTC became very moist. In fact, *a sizeable region of precipitable water (PW) over 5 cm was analyzed over southern Kansas (Fig. 13a), in which a_s > 3 in some areas (Fig. 13d)*. The standardized anomalies were large in the region where the MCS developed bow echo characteristics and accelerated to the east-southeast (Fig. 3e). Very high low-level moisture content is a common characteristic of severe, long-lived MCSs in both the warm and cool seasons (Johns and Hirt 1987; Johns 1993; Coniglio et al. 2004; Burke and Schultz 2004).

Also in contrast to the environment for the initial convective development was a region of very steep mid-level lapse rates (3 – 6 km lapse rates > 8.5 K km^{-1}) ahead of the maturing MCS (Fig. 14a). In fact, *the values of a_s > 4 for the lapse rates in far north central Oklahoma (Fig. 14d) were the largest standardized anomalies found for any variable at any time during the MCS development*. Consequently, *the very steep lapse rates and the high moisture content in the lowest 2 km AGL (Fig. 8) produced unusually large values of CAPE along the ensuing MCS path*, particularly in the few km above the level of free convection.

One of the motivations to study this event arose from the ability of the NOAA Storm Prediction Center to anticipate an unusually strong convective

wind event. The recognition of sufficient (although not unusually large) downdraft CAPE (DCAPE) to help organize convective outflows early in the convective event and sufficient mean flow/deep shear to organize the convective updrafts played a role in the forecast process. But the recognition of very high PW values and lapse rates in the downstream environment played a decisive role in the decision to issue a "Particularly Dangerous Situation" (PDS) Severe Thunderstorm Watch for this event, along with the recognition that a strong LLJ impinging on this area was likely to lead to an abundance of strong thunderstorms in a relatively confined region. Operational experience suggests that a high spatial concentration of thunderstorms commonly precedes the development of derechos.

Another interesting difference between the environment of the initial stages of the convection, and that ahead of the developing MCS, is the change in evaporative potential for convective downdrafts. Although the evaporation potential was sizeable during the pre-MCS stage of the event (prior to 0600 UTC) because of the dry, well-mixed boundary layer (Fig. 4), the DCAPE values in the immediate downshear environment after the development of the MCS were generally *less than* the typical DCAPE values for other MCS environments (Fig. 15). Although substantial dryness existed in the mid levels at 0500 UTC (Fig. 8), the relatively small lapse rates in the very moist surface – ~800 hPa layer, and the continued moistening of the mid-level environment throughout the evening, limited the magnitude of the DCAPE of the presumed downdraft parcels. Accordingly, available observations reveal the lack of a strong cold pool at the surface through 1200 UTC. Surface temperatures generally fell only 4 – 6 K after the passage of the convective line during its intense stages between 0900 and 1200 UTC (Figs. 3e and 3f). Surface temperature deficits were commonly much larger for the MCSs studied by Engerer et al. (2008) (likely because several daytime cases were included in their data set), but the temperature deficits of 4 – 6 K were similar to those found for the nocturnal bow echoes examined in Adams-Selin and Johnson (2010).

The finding of relatively small DCAPE and the lack of a strong cold pool at the surface strengthens one of the key arguments of this analysis: *The unusually high PW content and mid-level lapse rates suggest a primary role of the updraft strength in the ensuing development of the strong outflows. Given the modest evaporative cooling potential in the early mature stages of the MCS, and the abundant storm development in a relatively confined region over southeastern Kansas between 1000 and 1100 UTC (Fig. 1a), it is hypothesized that the melting and/or loading of the large volume of precipitation generated by the abundant, strong updrafts played a proportionally very large role in driving large downdraft mass fluxes and resulting strong outflows and severe surface winds*. Downdrafts are dependent on updrafts for the hydrometeors that drive them, through diabatic effects as well as precipitation drag (water loading). Thus, in a given thermodynamic environment, more updraft mass flux and, more specifically, more hydrometeor production tend to yield more downdraft mass flux. While parameters such as DCAPE may be useful for predicting the negative buoyancy potential for individual downdraft parcels that remain saturated, it seems likely that the intensity of low-level convective outflow is highly dependent on the volume of mass produced, regardless of the evaporative cooling effects from individual parcels. The recent modeling results of James and Markowski (2010) support this idea. They find several measures of convective system strength (total rainfall, total mass of each condensate species, and total updraft and downdraft mass fluxes) to generally increase as low- to mid-level dryness is lessened for the mid-latitude MCS environments modeled in their study.

4. SUMMARY AND CONCLUDING REMARKS

This study documents the development and early evolution of the remarkable derecho-producing MCS that traversed the central United States on 8 May 2009. The goal is to show that the evolution of the storms and the environment leading up to the development of the derecho was very complex, but the potential for a particularly severe convective wind event was signaled by strong anomalies in the pre-storm environment. Given the complexity of the convective evolution, and the departure it represents from the simpler environments that are the focus of the MCS modeling literature, unraveling the evolution that led to the severity of this event is no easy task. However examination of the anomalies in the environment and the evolving convective morphology yield important clues about the processes that shaped this event.

Initial convective development in northeast Colorado was fairly weak and unremarkable, but when outflow from some of these weaker storms began to lift slightly more unstable low-level air in western Kansas, a line of more intense convection developed. Meanwhile a deep layer of warm moist air surged northward out of Oklahoma and into the path of this initial line. Multiple features in the environment, possibly associated with air-mass boundaries along the leading edge of this surge, appeared to trigger several new convective lines in south-central and southeastern Kansas, including at least two bands with a distinctly different orientation than the initial line. Eventually, these components consolidated into a large MCS with a well-defined MCV and a strongly bowing convective line on the southeast flank. Although damaging winds were produced during the bowing stage of the system, a remarkable aspect of this event (but one that is not the focus of this study) was the very strong and long-lived MCV that persisted for several hours after the weakening of the main convective line.

The magnitude and geographical extent of severe winds associated with this event were anomalous compared to other MCSs. Yet, while the winds in the early evolution of the MCS were associated with convective downdrafts, commonly used methods to estimate the strength of convective downdraft outflow based on environmental

parameters did not yield unusually high values compared to other MCSs. Although the 0 – 6 km wind shear and mean wind speeds were certainly sufficient for organized severe convection and surface outflow, the values were not exceptionally large compared to other central plains MCS environments.

However, consideration of those environmental parameters that *were* unusual has important implications for predicting the strength of downdraft outflow, by virtue of what these parameters say about *updrafts*. For example, anomalously strong fields in this event included low-level storm inflow, PW, conditional instability, and inertial instability aloft. The combination of these multiple factors suggests that intense upward mass fluxes were strongly favored in this event – the potential energy supply was high, the relative humidity was high over deep layers (favoring minimal dilution of updrafts by entrainment), and an upper tropospheric environment was present that could accommodate massive detrainment of mass.

Why are these factors important for downdrafts? In a given thermodynamic environment, more updraft mass flux and, more specifically, more hydrometeor production tend to yield more downdraft mass flux. Therefore, factors that support large updraft mass fluxes in a concentrated area, such as the combination of high PW, a very strong and deep LLJ, and very steep lapse rates --- like those found in this study --- can also influence the strength of the convective downdrafts, regardless of the evaporation potential. This hypothesis for the 8 May 2009 derecho seems to be consistent with the results of James and Markowski (2010). They show that simulated MCSs generally become weaker as the low- to mid-level dryness is increased for the mid-latitude MCS environments modeled in their study. They explain that the increased entrainment of drier air into the updrafts reduces hail production and reduces the associated downdraft mass fluxes and outflow winds, and is a primary reason for the weaker MCSs.

To summarize, environmental parameters and observations of radar reflectivity indicate that an extraordinary amount of hydrometeors was available to drive downdrafts in the 8 May 2009 event. Even though the potential energy for individual downdraft parcels was not exceptionally large, it seems likely that the enormous updraft mass flux, resulting from a very strong and deep LLJ, very large lapse rates, and high PW in a confined area, led to high concentrations of hydrometeors that supported large downdraft mass fluxes, regardless of the evaporative potential. Water loading and/or the melting of abundant frozen hydrometeors aloft likely played an important role in producing the downdraft mass fluxes in this environment, since the evaporative potential was not exceptionally high. These processes are perhaps underappreciated in nocturnal severe wind-producing MCS events.

Acknowledgments. Part of the analysis presented here stemmed from discussions at the QLCS Advanced Warning Operations Course (AWOC) developer's workshop run by the NOAA/NWS Warning Decision Training Branch (WDTB). Participants included Dr. Nolan Atkins, Jeff Evans, Brad Grant, Jim LaDue, Les Lemon, Angela Lese, Steve Martinaitis, Dan Miller, Ron Przybylinski, Chris Spannagle, Pat Spoden, and Ray Wolf. A discussion with Dan Miller about the role of frontogenesis in MCS environments was helpful. Patrick Marsh helped with the interpretation of WSR-88D level II data in the Gibson Ridge GR2Analyst software. Greg Carbin inspired the authors to present the hourly composite reflectivity on one image (Fig. 1a). Jason Levit, Andy Dean, and Jay Liang archived the SPC operational data stream for this case, which allowed for an efficient perusal of the data for this study. Finally, we thank Dr. Matthew Parker for very thorough reviews of this manuscript and many helpful suggestions along the way, as well as Drs. David Stensrud, and Mace Bentley for helpful comments and suggestions on earlier versions of this manuscript.

REFERENCES

Adams-Selin, R. D., and R. H. Johnson, 2010: Mesoscale surface pressure and temperature features associated with bow echoes. *Mon. Wea. Rev.*, **138**, 212–227.

Atkins, N. T., and M. St. Laurent, 2009: Bow Echo Mesovortices. Part I: Processes that influence their damaging potential. *Mon. Wea. Rev.*, **137**, 1497–1513.

Benjamin, S. G., D. Devenyi, S. S. Weygandt, K. J. Brundage, J. M. Brown, G. A. Grell, D. Kim, B. E. Schwartz, T. G. Smirnova, T. L. Smith, and G. S. Manikin, 2004: An hourly assimilation-forecast cycle: The RUC. *Mon. Wea. Rev*., **132**, 495-518.

Blackadar, A. K., 1957: Boundary layer wind maxima and their significance for the growth of nocturnal inversions. *Bull. Amer. Meteor. Soc*., **38**, 283-290.

Blanchard, D. O., W. R. Cotton, and J. M. Brown, 1998: Mesoscale circulation growth under conditions of weak inertial instability. *Mon. Wea. Rev*., **126**, 118-140.

Bonner, W. D., 1968: Climatology of the low-level jet. *Mon. Wea. Rev*., **96**, 833-850.

Burke, P. C. and D. M. Schultz, 2004: A 4-yr climatology of cold-season bow echoes over the continental United States. *Wea. Forecasting*, **19**, 1061-1074

Coniglio, M. C., D. J. Stensrud, and M. B. Richman, 2004: An observational study of derecho-producing convective systems. *Wea. Forecasting*, **19**, 320-337.

----------, J. Y. Hwang, and D. J. Stensrud, 2010: Environmental factors in the upscale growth and longevity of MCSs derived from Rapid Update Cycle analyses. *Mon. Wea. Rev*., **138**, 3514-3539.

Cohen, A. E., M. C. Coniglio, S. F. Corfidi and S. J Corfidi, 2007: Discrimination of mesoscale convective system environments using sounding observations. *Wea. Forecasting*, **22**, 1045- 1062

Corfidi, S. F. 2003: Cold pools and MCS propagation: Forecasting the motion of downwind-developing MCSs. *Wea. Forecasting,* **18**, 997–1017.

Cotton, W. R., M. S. Lin, R. L. McAnelly, and C. J. Tremback, 1989: A composite model of mesoscale convective complexes. *Mon. Wea. Rev.*, **117**, 765–783.

Davis, C. A., and S. B. Trier, 2007: Mesoscale convective vortices observed during BAMEX. Part I: Kinematic and thermodynamic Structure. *Mon. Wea. Rev.*, **135**, 2029–2049.

Durran D. R., 1986: Mountain Waves. *Mesoscale Meteorology and Forecasting*, P. S. Ray, Ed., Amer. Meteor. Soc., 472-492.

Emanuel, K. A., 1979: Inertial instability and mesoscale convective systems. Part I: Linear theory of inertial instability in rotating viscous fluids. *J. Atmos. Sci*., **36**, 2425-2449.

Engerer, N. A., D. J. Stensrud, and M. C. Coniglio, 2008: Surface characteristics of observed cold pools. *Mon. Wea. Rev*., **136**, 4839- 4849.

Fujita, T. T., 1978: Manual of downburst identification for Project NIMROD. SMRP Res. Paper 156, University of Chicago, 104 pp.

Houze Jr., R. A., S. A. Rutledge, M. I. Biggerstaff, and B. F. Smull, 1989: Interpretation of Doppler weather radar displays of midlatitude mesoscale convective systems. *Bull. Amer. Meteor. Soc*., **70**, 608-619.

James, R. P., and P. M. Markowski, 2010: A numerical investigation of the effects of dry air aloft on deep convection. *Mon. Wea. Rev.*, **138**, 140–161.

Jirak, I. L. and W. R. Cotton, 2003: Satellite and radar survey of mesoscale convective system development. *Mon. Wea. Rev*., **131**, 2428-2449.

Johns, R. H., and W. D. Hirt, 1987: Derechos: widespread convectively induced windstorms. *Wea. Forecasting*, **1**, 32-49.

--------, 1993: Meteorological conditions associated with bow echo development in convective storms. *Wea. Forecasting*, 8, 294-299.

Laing, A. G., and J. M. Fritsch, 2000: The large-scale environments of the global populations of mesoscale convective complexes. *Mon. Wea. Rev.*, **128**, 2756–2776.

Maddox R. A., 1983: Large-scale conditions associated with midlatitude, mesoscale convective complexes. *Mon. Wea. Rev*., **111**, 1475-1493.

McAnelly, R. L., J. E. Nachamkin, W. R. Cotton, and M. E. Nicholls, 1997: Upscale evolution of MCSs: Doppler radar analysis and analytical investigation. *Mon. Wea.Rev.*, **125**, 1083-1110.

McNider, R. T. and R. A. Pielke, 1981: Diurnal boundary-layer development over sloping terrain. *J. Atmos. Sci.*, **38**, 2198-2212.

Miller, D. J., and R. H. Johns, 2000: A detailed look at extreme wind damage in derecho events. Preprints, *20th Conf. on Severe Local Storms*, Orlando, FL, Amer. Meteor. Soc., 52-55.

Orlanski, I., 1975: A rational sub-division of scales for atmospheric processes. *Bull. Amer. Meteor. Soc*., **56**, 527-530.

Parker, M. D., and R. H. Johnson, 2000: Organizational modes of midlatitude mesoscale convective systems. *Mon. Wea. Rev*., **128**, 3413-3436.

Schultz, D. M., and J. A. Knox, 2007: Banded convection caused by frontogenesis in a conditionally, symmetrically, and inertically unstable environment. *Mon. Wea. Rev*. **135**, 2095-2110.

Seman, C. J., 1994: A numerical study of nonlinear nonhydrostatic conditional symmetric instability in a convectively unstable atmosphere. *J. Atmos. Sci*., **51**, 1352-1371.

Szoke, E. J., M. L. Weisman, J. M. Brown, F. Caracena, and T. W. Schlatter, 1984: A Subsynoptic Analysis of the Denver tornadoes of 3 June 1981. *Mon. Wea. Rev.*, **112**, 790–808.

Tuttle, J. D., and C. A. Davis, 2006: Corridors of warm season precipitation in the central United States. *Mon. Wea. Rev.*, **134**, 2297–2317.

Uccellini, L. W., and D. R. Johnson, 1979: The coupling of upper and lower tropospheric jet streaks and implications for the development of severe convective storms. *Mon. Wea. Rev*., **107**, 682-703.

Vasiloff, S. V., D. J. Seo, K. W. Howard, J. Zhang, D. H. Kitzmiller, M. G. Mullusky, W. F. Krajewski, E. A. Brandes, R. M. Rabin, D. S. Berkowitz, H. E. Brooks, J. A. McGinley, R. J. Kuligowski, and B. G. Brown, 2007: Improving QPE and very short term QPF: An initiative for a community-wide integrated approach. *Bull. Amer. Meteor. Soc.*, **88**, 1899–1911.

Weisman, M. L., 1993: The genesis of severe, long-lived bow echoes. *J. Atmos. Sci*., **50**, 645-670.

Wheatley, D. M., R. J. Trapp, and N. T. Atkins, 2006: Radar and damage analysis of severe bow echoes during BAMEX. *Mon. Wea. Rev*., **134**, 791-806.

Zipser, E. J., 1982: Use of a conceptual model of the life cycle of mesoscale convective systems to improve very-short-range forecasts. *Nowcasting*, K. Browning, Ed., Academic Press, 191-221.